The effect of hydrogenation on magnetic interactions in CeNi

2009 J. Phys.: Condens. Matter 21 446003

(http://iopscience.iop.org/0953-8984/21/44/446003)

J. Phys.: Condens. Matter **21** (2009) 446003 (8pp) doi:10.1088/0953-8984/21/44/446003

The effect of hydrogenation on magnetic interactions in CeNi

A V Kolomiets[1,2], **L Havela**[1] **and J Pospíšil**[1]

[1] Department of Condensed Matter Physics, Faculty of Mathematics and Physics, Charles University, Ke Karlovu 5, 121 16, Prague 2, Czech Republic
[2] Department of Physics, National University 'Lvivska Polytechnica', Lviv, Ukraine

Received 10 August 2009, in final form 19 September 2009
Published 15 October 2009
Online at stacks.iop.org/JPhysCM/21/446003

Abstract
The crystal structure and magnetic properties of $CeNiH_{3.7}$ were studied by means of powder x-ray diffraction, specific heat, and dc and ac magnetization techniques. It was established that hydrogenation stabilizes the $4f^1$ state of Ce and turns CeNi–H into a dilute Kondo system with $T_K = 3.7$ K. The Kondo screening in $CeNiH_{3.7}$ is suppressed by the applied magnetic field, although it still affects the properties of $CeNiH_{3.7}$ at 14 T, as indicated by the enhanced γ-coefficient of electronic specific heat, which remains more than twice as large as in the precursor compound CeNi. Its zero-field value is as high as 1890 mJ (mol $K^2)^{-1}$. Hydrogenation acts primarily as the negative pressure agent in $CeNiH_{3.7}$, while the role of H–metal bonding is secondary.

1. Introduction

Ce-based intermetallic compounds are attracting permanent attention due to their broad variety of physical properties [1], originating from the changing character of Ce 4f electronic states. This can be from atomic-like to almost itinerant, depending on the crystal structure and the 4f–ligand hybridization. Both of these parameters can be further tuned by application of external pressure [2] or hydrogenation, which expands the crystal lattice [3] (but can also modify bonding conditions) and thus resembles negative pressure.

Intermetallic compound CeNi is a paramagnet, in which the cerium atoms have non-integer f-state occupancy (n_f) and the nickel atoms do not carry any magnetic moments [4–7]. The non-integer value of n_f for cerium in this compound means that the states corresponding to the $4f^1$ and $4f^0$ configurations are close to the Fermi level ε_F and to each other, which results in the mixing of these states due to electronic fluctuations. The 4f-spectral density was studied by resonant photoemission [8], revealing a spectral peak due to hybridization between the 3d-states of Ni and 4f-states of Ce at 2.7 eV below ε_F. Such density of electronic states makes the physical properties of CeNi sensitive to volume modification. Indeed, the application of external pressure to CeNi leads to a first-order phase transition analogous to the γ–α transition in Ce already at $p =$ 5 kbar [9], and suppresses spin fluctuations [10]. Based on that, one can expect that hydrogenation, which is a complementary technique to the external pressure, can promote a stabilization of local Ce moments.

The first report on the synthesis of CeNi hydride with $CeNiH_{3.7}$ stoichiometry came from Verbetskii and co-workers, who investigated the synthesis conditions and the crystal structure of various $RNiH_x$ (R = rare-earth metal) compounds [11]. The pilot studies of the magnetic properties of the CeNi hydride with 2.9 hydrogen atoms/f.u. indicated that in this compound $n_f = 1$ ($4f^1$ state) but the ground state remains paramagnetic [12].

In the present paper we report on a detailed study of $CeNiH_{3.7}$, which shows that after a hydrogenation, leading to a substantial volume increase, the Kondo lattice CeNi transforms into a dilute Kondo system $CeNiH_{3.7}$ with the Sommerfeld coefficient of the electronic specific heat $\gamma(0\ \mathrm{T}) = 1.89$ J (mol $K^2)^{-1}$.

2. Experimental details

CeNi was melted from Ce of the 3N and Ni of 4N purity in a monoarc furnace filled with the 6N purity argon gas. In order to ensure the homogeneity, the ingots were turned and remelted several times. After the melting they were sealed in evacuated quartz tubes, annealed at 450 °C for 1 week and slowly cooled down to room temperature. The crystal structure was examined by powder x-ray diffraction (Cu Kα radiation, Bragg–Brentano setup). The same diffraction apparatus was used for structure studies of the hydrides.

Prior to hydrogenation, the ingot was crushed into sub-millimetre particles and the surface of the material was

Table 1. Details of the atomic structure of $CeNiH_{3.7}$ (CrB-type structure, space group *Cmcm*). (Note: Bragg *R*-factor 8.2, RF-factor 6.7.)

				Atomic positions			
				Ce		Ni	
a (Å)	3.9304(7)	$\Delta a/a$ (%)	4.7	4c		4c	
b (Å)	11.889(1)	$\Delta b/b$ (%)	12.4	*x*	0	*x*	0
c (Å)	4.8440(7)	$\Delta c/c$ (%)	10.7	*y*	0.1307	*y*	0.4089
		$\Delta V/V$ (%)	30.3	*z*	1/4	*z*	1/4

activated by 2 h annealing at 250 °C and a pressure of 10^{-6} mbar. After cooling down, 0.8 bar of the hydrogen gas (6N purity) was introduced into the reaction chamber. Subsequent reaction led to a pressure drop on the timescale of minutes, but the sample was exposed to H_2 for several hours to reach full equilibrium. The crystal structure of the product obtained was then examined by x-ray diffraction.

Specific heat and magnetization measurements were performed on a commercial PPMS Quantum Design setup equipped with a 14 T magnet. The samples for the specific heat experiments were obtained by compressing very fine $CeNiH_{3.7}$ powder into pellets. Typical pressures used for the pellet production were 2–5 kbar. The samples for magnetization were obtained by fixing grains of the same powder in random positions by a small amount of an acetone-soluble glue (diamagnetic).

3. Experimental results

3.1. Hydrogen content and crystal structure

The composition of the hydride was determined both by the volumetric method based on the pressure drop in the calibrated volume and by monitoring the amount of hydrogen, which was released from the CeNi hydride during the decomposition in vacuum. The results of both techniques were in good agreement and yielded a hydrogen content of (3.7 ± 0.3) H atoms/f.u.

The x-ray diffraction (XRD) study revealed that, except for several minor peaks of cerium oxide observed at low diffraction angles, the pattern corresponds to that of expanded CeNi. The atomic parameters of $CeNiH_{3.7}$ obtained from the Rietveld refinement (see table 1) are consistent with the results reported earlier [11–14], including the atomic positions of Ce and Ni. The discrepancy between the present results and those reported in the literature is within the error limits typical for the hydride formation.

The relative increase of the unit cell volume due to the hydrogenation is $\Delta V/V = 30.3\%$. Yet, in spite of the substantial lattice expansion, the metal atoms in $CeNiH_{3.7}$ form the same crystal structure as in the parent compound, i.e. the orthorhombic CrB-type structure (space group *Cmcm*). X-ray diffraction does not provide any information regarding the positions of the hydrogen atoms due to their small scattering cross-section. As can be seen from the table 1, the lattice expansion is anisotropic: it takes place mainly along the *b* and *c* axes, whereas the relative increase $\Delta a/a$ is 2.5 times smaller than $\Delta b/b$. The anisotropic lattice expansion affects also the nearest neighbour coordination of the atoms. Particularly, in CeNi the nearest neighbours of cerium are Ni atoms. The Ce–Ni distance in the parent compound is $d_{Ce-Ni} = 2.96$ Å while the Ce–Ce distance is notably larger: $d_{Ce-Ce} = 3.73$ Å. After the hydrogen absorption, the interatomic spacing changes as follows: $d_{Ce-Ni} = 3.15$ Å (+6.1%) and $d_{Ce-Ce} = 3.93$ Å (+5.4%). The enhanced Ce–Ni distances suggest that the 4f–3d hybridization should be weaker in $CeNiH_{3.7}$ than in CeNi.

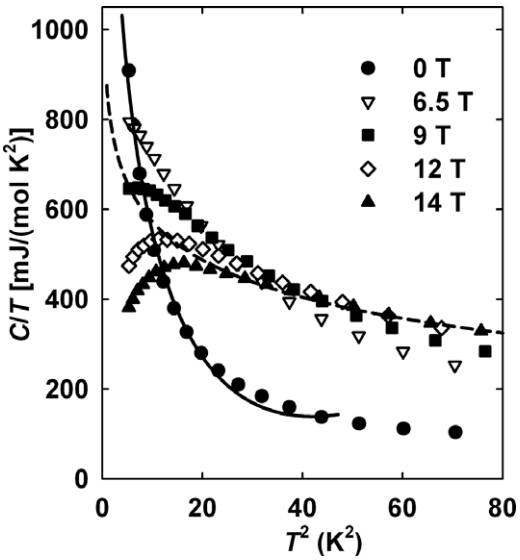

Figure 1. Low-temperature specific heat of $CeNiH_{3.7}$ in various magnetic fields. The solid and dashed lines indicate the fits of the experimental data collected at 0 T and 14 T, respectively, by equation (3).

3.2. Specific heat

The specific heat of $CeNiH_{3.7}$ was studied in magnetic fields up to 14 T and in the temperature range from 2 to 300 K. The measured $C(T)$ curves show pronounced field sensitivity below 20 K (figure 1), while above this temperature there is hardly any difference between the data sets collected in different magnetic fields. Figure 1 shows the $C/T(T^2)$ data only up to $T^2 = 80$ K^2 ($T \approx 9$ K) where the field sensitivity is the most pronounced. The specific heat monotonously decreases with decreasing temperature from $T = 300$ down to 20 K (figure 2), then, at about 10 K, a minimum is observed on the $C(T)$ curves and the further decrease of temperature leads to an increase of the $C(T)$ values. Specific heat at the lowest experimentally available temperature is unusually high (of the order of 1000 mJ (mol K^2)$^{-1}$) for a conventional metallic system, indicating the enhanced electronic contribution.

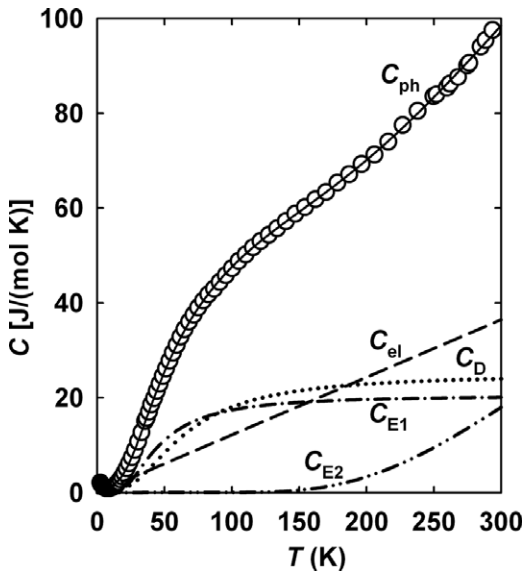

Figure 2. Specific heat of $CeNiH_{3.7}$ up to 300 K. The solid line indicates the fit of the experimental data by $C = C_{\rm el} + C_{\rm Debye} + C_{\rm Einstein}$. The contributions of the individual electronic, Debye, and Einstein terms are shown as well.

For the analysis of the electronic term in the specific heat, the lattice contributions should be approximated as precisely as possible. Here we use a simplified analysis, assuming the presence of the acoustic and optical branches in the phonon spectrum and neglecting possible thermal expansion effects and/or H diffusion at elevated temperatures, possibly contributing to the $C(T)$ upturn for $T > 250$ K. We have found that from 25 to 200 K the $C(T)$ data can be fairly well described by the following expression:

$$C = C_{\rm el} + C_{\rm Debye} + C_{\rm Einstein} \tag{1}$$

where $C_{\rm el}$, $C_{\rm Debye}$, and $C_{\rm Einstein}$ are electron, Debye, and Einstein terms, respectively. We assumed the following expression for the analysis of $C(T)$ in the temperature range $T > 20$ K:

$$C = \gamma_0 T + 9R\left(\frac{T}{\Theta_{\rm D}}\right)^3 \int_0^{\frac{\Theta_{\rm D}}{T}} \frac{x^4 {\rm e}^x}{({\rm e}^x - 1)^2}{\rm d}x + R\sum_i n_{{\rm E}i}\left(\frac{\Theta_{{\rm E}i}}{T}\right)^2 \frac{{\rm e}^{\Theta_{{\rm E}i}/T}}{({\rm e}^{\Theta_{{\rm E}i}/T} - 1)^2} \tag{2}$$

where γ_0 is the electron coefficient, $\Theta_{\rm D}$ the Debye temperature, $\Theta_{{\rm E}i}$ the Einstein temperature of the ith optical phonon branch, $n_{{\rm E}i}$ the degeneracy of the ith optical phonon branch, and R the gas constant. We considered the lattice specific heat of $CeNiH_{3.7}$ consisting of three acoustic and 15 optical branches. In an ideal unit cell with six atoms the sum of all $n_{{\rm E}i}$ should be equal to 15. In order to keep the number of fitting parameters as small as possible, only one Debye temperature was used for all three acoustic branches or, in other words, the acoustic part of the phonon spectrum was considered to be three-fold degenerate.

Figure 2 shows the zero-field specific heat of $CeNiH_{3.7}$ fitted to equation (2). Disregarding the low-temperature upturn, the calculations yield the following parameters: $\gamma_0 = 121$ mJ (mol K^2)$^{-1}$, $\Theta_{\rm D} = 264$ K, $\Theta_{\rm E1} = 140$ K, and $\Theta_{\rm E2} = 1495$ K. The electronic contribution to the specific heat described by the γ_0-term is much higher than expected for a conventional metallic system, indicating an enhancement of the density of states at the Fermi level. The difference of one order of magnitude between the two $\Theta_{\rm E}$ values can be attributed to the oscillations in two subsystems: the crystal lattice built from the relatively heavy metal atoms of Ce and Ni, and much lighter hydrogen atoms filling the interstitials. The zero-field value of the specific heat reaches 94 J (mol K)$^{-1}$ at $T = 300$ K, and yet it remains at room temperature even below the Dulong–Petit limit, which is 149 J (mol K)$^{-1}$ for the six-atom unit cell, and further increase can be expected at elevated temperatures.

As mentioned above, the specific heat of $CeNiH_{3.7}$ reaches a minimum at approximately 10 K, below which it increases with decreasing temperature. This feature is emphasized by plotting the data as C/T versus T^2 (figure 1). With the increase of the applied magnetic field, the low-T upturn on the $C/T(T^2)$ curve levels off and shifts towards higher temperatures. Starting from $\mu_0 H = 9$ T, a maximum forms on the C/T versus T^2 curve, and the further increase of H results in the displacement of the maximum towards higher temperatures. Such behaviour can correspond to different scenarios such as the Kondo effect, non-integer $n_{\rm f}$, etc, which can be plausible for $CeNiH_{3.7}$. The difference between the curve shapes, attributed to these phenomena sometimes is rather small, especially when fitting the data across a decade of temperature or less as it is in the present case. That is why we sought a model which could properly describe the low-T upturns in all the fields studied.

To analyse the upturn, we tentatively used all models, which may yield such a type of $C(T)$ curve shape. The analytic expressions corresponding to the Schottky anomaly, intermediate valence state, or quasi-paramagnetic state, were used to fit the experimental data, and in a certain range of magnetic fields their agreement with experimental data was rather good. Yet it was found that the best correspondence between the experimental and calculated data sets for all fields is achieved when the Kondo-term is included in the expression for the specific heat:

$$C = C_{\rm el} + C_{\rm Debye} + C_{\rm Kondo}. \tag{3}$$

The term $C_{\rm Kondo}$ was taken in the form $C_{\rm Kondo} = -\delta T \ln(T/T_{\rm K})$, and the Einstein term of the lattice specific heat was not taken into consideration since the contributions of the Einstein modes are negligibly small in the temperature range of the fit, i.e. for $T < 10$ K. Such simplification has proved to be justified since the $\Theta_{\rm D}$ values obtained by fitting the low-T specific heat were in good agreement with the Debye temperature used to describe the high-temperature data (25–300 K).

Equation (3) was successfully used to model the specific heat anomalies observed in all fields from 0 to 14 T. The temperature range, across which equation (3) is valid, shifts towards higher temperatures with increasing field. Two of the fitting curves (for 0 and 14 T) are shown in figure 1 in order

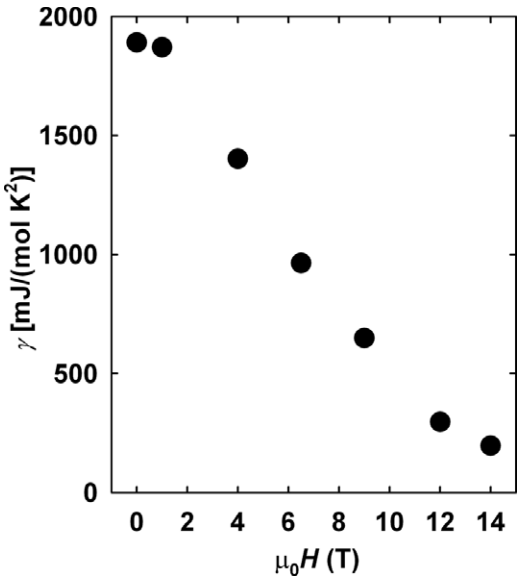

Figure 3. Field dependence of the coefficient of electronic specific heat γ obtained from the fits at low temperatures.

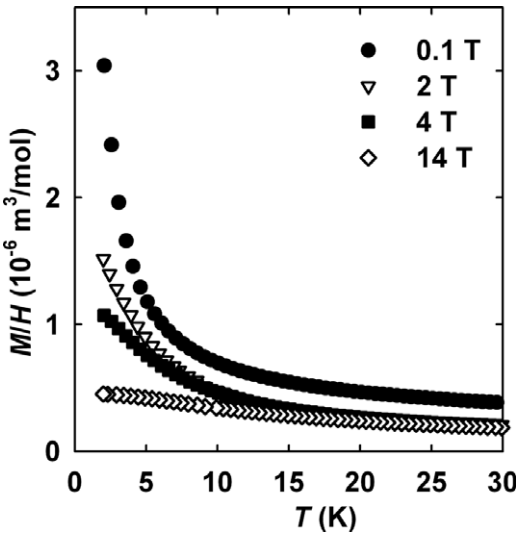

Figure 4. Temperature dependence of the low-temperature magnetic susceptibility of $CeNiH_{3.7}$. Higher values of susceptibility in low fields are due to a small amount of ferromagnetic impurity with high Curie temperature.

to illustrate the quality of the fit. The other calculated curves show similar coincidence with the measured data points. All of them give the same value of the Kondo temperature: $T_K = (3.7 \pm 0.3)$ K. On the contrary, the electronic coefficient γ and the scaling coefficient δ were found to be field dependent. The coefficient δ monotonously decreases with increasing field from 2.4 J (mol K^2)$^{-1}$ at 0 T down to 0.7 J (mol K^2)$^{-1}$ at 14 T, indicating the suppression of the Kondo screening by magnetic field. The electronic coefficient γ also decreases when the field goes up (figure 3). The γ-value changes by an order of magnitude from $\gamma(0\ \text{T}) = 1890$ J (mol K^2)$^{-1}$ to $\gamma(14\ \text{T}) = 197$ J (mol K^2)$^{-1}$. The latter value is already close to the high-temperature $\gamma_0 = 121$ mJ (mol K^2)$^{-1}$ given above.

3.3. Magnetization

The first magnetization study of the CeNi hydride was reported in [12]. Namely, it was a temperature scan of the magnetic susceptibility of $CeNiH_{2.9}$ in a field of $\mu_0 H = 4$ T. According to [12], the CeNi hydride is a paramagnet with Curie–Weiss behaviour, its effective moment is close to the value corresponding to the $4f^1$ configuration of Ce, and the paramagnetic Curie temperature $\Theta_p = -19$ K. To our knowledge, no other magnetization experiments had been performed on CeNi hydrides. Such a situation motivated us to perform a more thorough study.

Hydrogenation of CeNi results in the enhancement of magnetic susceptibility: it becomes more than an order of magnitude larger in $CeNiH_{3.7}$ compared to the hydrogen-free CeNi [5, 15], which has a broad maximum at temperatures around 150 K. The susceptibility of the hydride is monotonous, following the Curie–Weiss law and deviating towards higher values in the low-T range (figures 4 and 5). This upturn, which cannot be fully accounted for by the Curie–Weiss law, and which flattens out with the increasing field, can be approximated by an additional logarithmic dependence

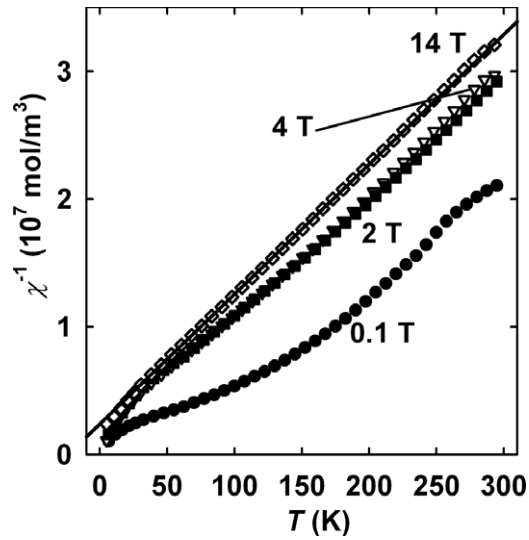

Figure 5. Inverse susceptibility of $CeNiH_{3.7}$ measured in various magnetic fields. The solid line corresponds to the Curie–Weiss fit of the data for $\mu_0 H = 14$ T. The irregular shape for low fields is due to the ferromagnetic impurity.

$\chi = M/H \propto -T \ln(T/T_K)$ as expected for the Kondo system. The temperature range, across which this analytic expression can be used, is broader compared to the specific heat data. For example, for $\mu_0 H = 14$ T the magnetization data follow the $-T \ln(T/T_K)$ dependence up to $T = 30$ K whereas the specific heat data at the same field can be accounted for by equation (3) only up to $T = 15$ K. The Kondo temperature values obtained from the susceptibility analysis are consistent with the $T_K = 3.7$ K coming from the specific heat curve, although it should be noted that the T_K values in the former case vary with field from $T_K(0.1\ \text{T}) = 5.2$ K to $T_K(14\ \text{T}) = 1.1$ K. Other reasons for the upturn could be crystal-field or spin-fluctuation effects. In addition, a spurious Curie term,

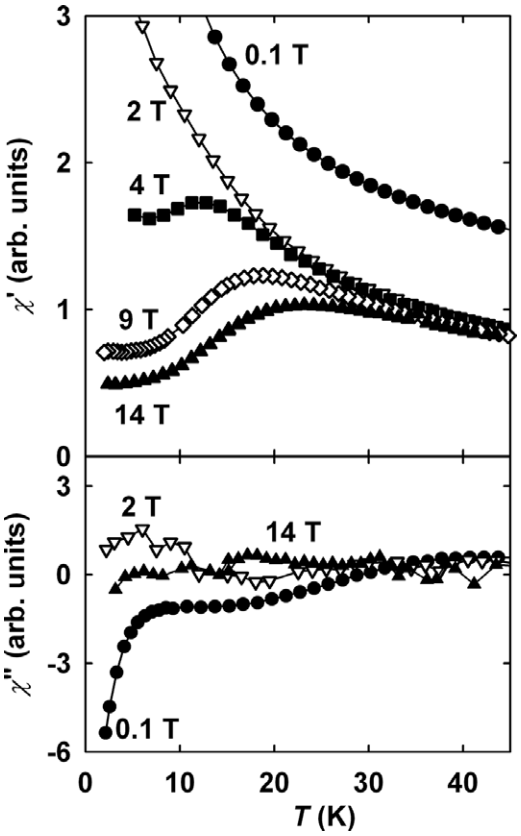

Figure 6. Real χ' and imaginary χ'' parts of the ac susceptibility of $CeNiH_{3.7}$ as measured in various dc magnetic fields. Lines are guides to the eye.

originating from a small admixture of magnetic rare earths, can be generally expected to appear in this temperature range, too, making a detailed quantitative analysis difficult.

The comparison of the high-temperature part of susceptibility measured in various fields indicates the presence of a small amount (on the ppm level, i.e. not observable by x-ray diffraction) of some ferromagnetic impurity with the Curie temperature exceeding the room temperature. For an analysis of the Curie–Weiss behaviour we, therefore, used the 14 T data set, which is least affected by the impurity magnetization. It was found that the magnetic susceptibility of $CeNiH_{3.7}$ follows the Curie–Weiss dependence:

$$\chi = \frac{C}{(T - \Theta_p)} \tag{4}$$

from 30 to 300 K (figure 5). The effective moment per atom is $\mu_{eff} = 2.5\ \mu_B$/f.u. and the paramagnetic Curie temperature $\Theta_p = -24$ K. Since nickel atoms in CeNi do not carry any magnetic moment [6], the same can be assumed also for the hydride. Then $\mu_{eff} = 2.5\ \mu_B$/f.u. found for $CeNiH_{3.7}$ will be the effective moment of Ce, and this value is very close to $\mu_{eff} = 2.54\ \mu_B$/f.u. calculated from Hund's rules for Ce^{3+}.

In order to check for a possible magnetic phase transition, which could have been missed in the $M(T)$ scans, we also performed ac magnetization measurements of $CeNiH_{3.7}$ in various dc fields. The results of the temperature scans of χ_{ac} are shown in figure 6. There are no anomalies pointing to the magnetic ordering on the measured curves. The $\chi'(T)$ curves measured at $\mu_0 H = 0.1$ and 2 T monotonously increase with increasing temperature down to the lowest experimentally available temperature of 2 K. The broad maximum, which starts to develop in a field of 4 T is related to the gradual curving of the $M(H)$ curves with decreasing T, as $\chi'(T)$ reflects the field derivative of magnetization in a given dc field. No features can be associated with a possible spin-glass behaviour indicated, for example, in the isostructural $CeNi_xCu_{1-x}$ [16].

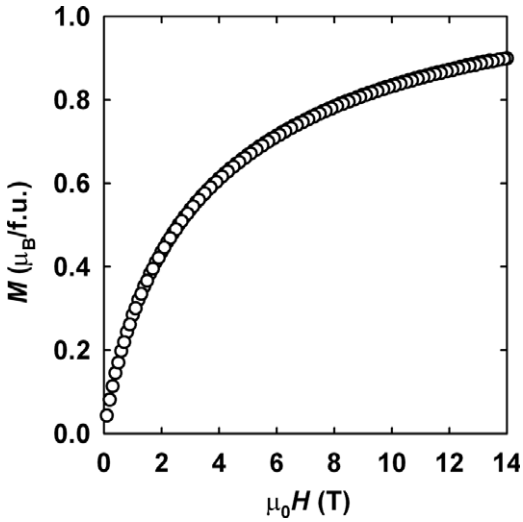

Figure 7. Field dependence of magnetization of $CeNiH_{3.7}$ measured at $T = 2$ K.

Finally, the field dependence of the dc magnetization $M(H)$ was measured at $T = 2$ K (figure 7). It monotonously increases up to the maximal experimentally available field $\mu_0 H = 14$ T. The low-field curvature of $M(H)$ together with the deviation of the inverse susceptibility $\chi^{-1}(T)$ from the straight line (figure 5) may indicate the presence of some ferromagnetic impurity. No hysteresis was observed. The experimental $M(H)$ curve goes well below the magnetization calculated according to the Brillouin function assuming the saturation moment of 2.14 μ_B/Ce. Among the possible explanations of the observed discrepancy between the curves are Kondo screening of the 4f moments or the crystal-field effects.

4. Discussion

The hydride of the $CeNiH_{3.7}$ stoichiometry studied in the present work was synthesized at a hydrogen pressure of $p_{H2} < 1$ bar and room temperature. The hydrogenation of CeNi resulted in about 30% expansion of the crystal lattice, yet the material did not lose its crystallinity. The increase of temperature above 523 K and the pressure up to $p_{H2} = 60$ bar led to the formation of the binary hydride CeH_x. In our opinion, the decomposition of CeNi during the hydrogenation is mainly due to the increase of temperature, and not of the hydrogen pressure. This can be

corroborated by the earlier reports on the $CeNiH_x$ synthesis at elevated pressures [11, 12, 14], which indicate that CeNi does not decompose in hydrogen at pressures as high as $p_{H2} = 60$ bar when the absorption takes place at room temperature. On the other hand, at higher temperature CeNi decomposes into CeH_3 and $CeNi_5$ in an H_2 atmosphere [11]. Hence, one can conclude that the temperature is the main parameter that determines whether CeNi is decomposed during the hydrogenation process, yielding a binary Ce hydride, or not; and the applied hydrogen pressure mainly influences the amount of hydrogen that is absorbed by the sample. The best route for the $CeNiH_x$ synthesis is the application of low hydrogen pressure ($p_{H2} \leqslant 1$ bar) at moderate temperature.

Due to the small atomic number Z the hydrogen atoms do not contribute to the intensities in XRD patterns. Therefore, the x-ray diffraction cannot provide any direct information on H atomic positions. Still, certain assumptions can be drawn from the analysis of the non-isotropic distortions of the host crystal lattice produced by the hydrogenation. Based on such an analysis of the XRD pattern of $CeNiH_{2.9}$ Bobet *et al* [12] have suggested the following positions for hydrogen: (1) the 8f site of the *Cmcm* space group (Ce_3Ni tetrahedra); (2) the 4c site (trigonal bypiramide Ce_3Ni_2). The same structure model was proposed for isostructural $ZrNiH_{3.0-\delta}$ [17, 18], yet the complete filling of both 8f and 4c sites would give the $CeNiH_{3.0}$ stoichiometry while the hydrogen content reported in [11] as well as that achieved in the present work is higher, namely 3.7 H atoms/f.u. This indicates that additional crystallographic sites should be occupied by hydrogen in order to reach a composition exceeding 3 H atoms/f.u. The 4a position was suggested earlier for the isostructural PrNi hydride (Ce_2Ni_4 octahedra) [14]. Alternatively, five possible interstitial sites, which can be occupied by hydrogen in the orthorhombic *Cmcm* structure, were proposed by Westlake [19]. To resolve this issue, a neutron diffraction experiment is required to determine the exact location of the hydrogen atoms in $CeNiH_x$ with $x > 3.0$.

The analysis of the specific heat and magnetization data for $CeNiH_{3.7}$ indicate that hydrogenation of CeNi affects the f-state occupancy in Ce, that is the n_f changes from a non-integer value [6, 7] to $n_f = 1$ ($4f^1$). The concomitant effect is suppression of spin fluctuations, which are driven by the charge fluctuations between the $4f^0$ and $4f^1$ configurations in CeNi. Their role is overtaken by the Kondo effect in the hydride where the $4f^1$ configuration is stabilized. The Kondo screening also produces a large enhancement of the electronic contribution to the specific heat.

The development of the Kondo state (with generally higher γ-values than for Ce with a non-integer n_f) in $CeNiH_{3.7}$ is indicated by the γ-enhancement. Even if the specific heat data above $T = 25$ K are used for the determination of the γ coefficient, one arrives at $\gamma_0 = 121$ mJ (mol K^2)$^{-1}$ for the hydride. This is by almost 50% higher than the value reported for CeNi: $\gamma_0 = 85$ mJ (mol K^2)$^{-1}$ [20].

The specific heat data below $T = 25$ K show the features, which are typical for the Kondo system: specific heat has a logarithmic upturn; the γ-value determined in the temperature range $T < 10$ K is as high as 1890 mJ (mol K^2)$^{-1}$; the $C(T)$ upturn transforms into a broad $C/T(T^2)$ maximum in higher fields ($\mu_0 H \geqslant 9$ T). If magnetic field is increased above 9 T, this maximum is suppressed but survives at least up to $\mu_0 H = 14$ T, which points to rather robust magnetic correlations. The modification of the $C(T)$ maximum with applied field follows the prediction for the thermodynamic properties of the diluted Kondo system [21]. The Kondo temperatures determined from the specific heat data in different magnetic fields are quite similar and fall within the range of $T_K = (3.7 \pm 0.3)$ K.

The conclusion about the Kondo regime in $CeNiH_{3.7}$ is corroborated by the magnetization studies. Namely, the dc susceptibility χ (in our case $\chi = M/H$) shows the same logarithmic divergence as the specific heat: $\chi \propto C \propto -T \ln(T T_K)$. Moreover, the T_K values obtained from the susceptibility fits and ranging from 1 to 5 K are consistent with $T_K = 3.7$ K obtained from fitting the specific heat data.

Certain insight into the mechanism through which the hydrogenation affects the magnetic interactions in CeNi can be obtained by comparing the properties of $CeNiH_{3.7}$ with those of the hydrogen-free derivatives of CeNi having the expanded crystal lattice.

The substitution of nickel for copper in $CeNi_{1-x}Cu_x$ stabilizes the $n_f = 1$ occupancy in Ce, and $CeNi_{1-x}Cu_x$ becomes a heavy-fermion compound with short-range correlations [22–24]. The change of properties is attributed to the decrease of the hybridization between the cerium 4f-states and the conduction band [23]. The increase of the lattice volume with Cu doping is rather moderate (compared to the hydrogenation): $\Delta V/V = +1.7\%$ for $CeNi_{0.85}Cu_{0.15}$ [22, 25].

The alloying with Pt in $CeNi_{1-x}Pt_x$ also stabilizes the $n_f = 1$ occupancy in Ce and facilitates magnetic interactions turning the paramagnet CeNi into the ferromagnetically ordered dense Kondo system $CeNi_xPt_{1-x}$ with a crossover concentration of about $x = 0.9$ [26, 27]. The lattice expansion accompanying the Pt doping is rather large, e.g. $\Delta V/V = 8.3\%$ for $x = 0.5$ [26], yet it is the Pt 5d to Ce 5d electron transfer that is considered to be the main factor in reducing the 4f-conduction band hybridization and the subsequent change of the magnetic interactions in $CeNi_xPt_{1-x}$ [26, 27].

Certain parallels can be drawn between the hydrogenation of CeNi and diluting the Ce sublattice with La in $Ce_{1-x}La_xNi$: in both cases the density of the 4f-states at the Fermi level is reduced, the same holds for the 4f-conduction band hybridization. Indeed, the decrease of the Ce concentration in $Ce_{1-x}La_xNi$ hinders the 4f–3d hybridization, leads to a monotonous decrease of the Kondo temperature, and $Ce_xLa_{1-x}Ni$, consequently turns into the dilute Kondo system [20, 28–30]. The specific heat curves of $Ce_xLa_{1-x}Ni$ in the Kondo impurity regime [20, 29] are very similar to those obtained for $CeNiH_{3.7}$. The volume expansion accompanying La doping is rather moderate: at a crossover concentration of $x = 0.6$ the unit cell volume of $Ce_xLa_{1-x}Ni$ is by approximately 3% larger than that of CeNi [30].

In all the cases cited above the weaker 4f-conduction band hybridization favours the $n_f = 1$ occupancy in Ce. Also the population of the 5d band of Ce promotes the magnetic ordering.

Based on analysis of the experimental data for $CeNiH_{3.7}$ as well as the effect of alloying CeNi with d- and f-metals, one can conclude that the volume increase due to the hydrogenation plays the dominant role in reducing the 4f-hybridization with non-f-states in CeNi amounting to increasing stability of the Ce 4f-states. The change of the electronic density due to hydrogen bonding has a secondary role even though H tends to behave as an anionic dopant in the presence of the strongly electropositive Ce. The Pt or Cu substitutions in CeNi, which are similar to the hydrogen bonding in the sense that they lead to the redistribution of the electronic density between the d-bands of Pt(Cu) and Ni, are supporting the long-range magnetic order. In contrast, the La doping, which does not affect the d-electron density, results in the dilute Kondo state. Moreover, the properties of $CeNiH_{3.7}$ and $Ce_{0.2}La_{0.8}Ni$ [20, 29] are rather similar.

Finally, the high-pressure studies of CeNi reported in [9] are completing the picture concerning the role of the volume changes in CeNi: in this compound the Ce 4f-states are delocalized at $p = 1.3$ kbar through the first-order phase transition. Rather low critical pressure points to the proximity of the 4f-states to the Fermi level and substantial hybridization between the 4f and conduction electron states. Hence, one can conclude that the magnetic properties of CeNi should be sensitive to volume changes, and that the hydrogenation plays the role of the negative pressure agent in CeNi.

It is likely, though, that the Kondo impurity regime sets in $CeNiH_x$ well before the 30% lattice expansion corresponding to a hydrogen concentration of $x = 3.7$ is reached. As shown in [30], $Ce_xLa_{1-x}Ni$ turns into the dilute Kondo system already at $\Delta V/V = 2.3\%$, and its Kondo temperature reaches $T_K = 5$ K at $\Delta V/V = 6.3\%$. Possibly, a similar situation takes place in $CeNiH_x$: the diluted Kondo regime is established at low hydrogen concentration and the further lattice expansion does not affect the location of CeNi on the Doniach diagram.

The increase of the 4f-localization in cerium due to hydrogenation is one of the two typical routes observed for Ce-based compounds. The incorporation of hydrogen into the crystal lattice acts either like negative pressure, which stabilizes the f-occupancy in Ce (CeNiGa–H [31], CeRhSn–H, CeIrS–H [32]), and in some cases induces magnetic order (CeNiIn–H [33], CeRuSi–H [34, 35]); or alternatively, the Ce–H bonding prevails and the magnetic order is destroyed (CeCoSi–H [36, 37], CeCoGe–H [37, 38]). Even more diversity of reactions to the hydrogenation can be added by a variable disorder introduced by incomplete occupation of the equivalent H sites. The disorder can come into action also in $CeNiH_{3.7}$ due to non-integer occupancy of H site(s). It can be associated with some of the features observed, as a contribution to the low-temperature susceptibility upturn can be expected from cerium in the full $4f^1$ state. A distribution of Ce atoms with slightly different n_f occupancies, and hence with different Kondo temperatures, is also considered as one reason for the occurrence of the logarithmic divergence of magnetic susceptibility [39].

5. Conclusions

Hydrogenation affects the crystal structure and magnetic properties of CeNi. CeNi readily absorbs hydrogen in a broad range of pressures, although high absorption capacity can be achieved even at room temperature and hydrogen pressures p_{H2} less than 1 bar. The CrB-type structure of the parent compound is preserved in the hydride $CeNiH_{3.7}$ despite the unusually high volume increase of $\Delta V/V = 30.3\%$. From the point of view of electronic structure the hydrogenation of CeNi can be considered primarily as the negative pressure effect, whereas the role of the Ce–H bonding is weak. The specific heat and magnetization studies indicate that upon hydrogen uptake CeNi turns effectively into a dilute Kondo system with $T_K = 3.7$ K. The properties may be affected by disorder.

Acknowledgments

This work was supported by the Grant Agency of the Czech Republic, grant No. 202/07/0418. This work is a part of the research plan MSM 0021620834 financed by the Ministry of Education of the Czech Republic.

References

[1] Sereni J G 1991 Low-temperature behaviour of cerium compounds *Handbook on the Physics and Chemistry of Rare Earths* vol 15, ed K A Gschneidner Jr and L Eyring (Amsterdam: Elsevier Science BV) p 1
[2] Thompson J D and Lawrence J M 1994 High pressure studies—physical properties of anomalous Ce, Yb and U compounds *Handbook on the Physics and Chemistry of Rare Earths* vol 19, ed K A Gschneidner Jr, L Eyring, G H Lander and G R Choppin (Amsterdam: Elsevier Science BV) p 383
[3] Wiesinger G and Hilscher G 2008 Magnetism of hydrides *Handbook of Magnetic Materials* vol 17, ed K H J Buschow (Amsterdam: Elsevier BV) (Magnetism of Hydrides) p 293
[4] Gignoux D, Givord F, Lemaire R and Tasset F 1983 *J. Less-Common Met.* **94** 165
[5] Fillion G, Gignoux D, Givord F and Lemaire R 1984 *J. Magn. Magn. Mater.* **44** 173
[6] Gignoux D, Givord F, Lemaire R and Tasset F 1985 *J. Magn. Magn. Mater.* **50** 53
[7] Clementyev E S, Mignot J M, Alekseev P A, Lazukov V N, Nefeodova E V, Sadikov I P, Braden M, Kahn R and Lapertot G 2000 *Phys. Rev.* B **61** 6189
[8] Kashiwakura T, Suzuki S, Okane T, Sato S, Kinoshita T, Kakizaki A, Ishii T, Isikawa Y, Yamagami H and Hasegawa A 1993 *Phys. Rev.* B **47** 6885
[9] Gignoux D and Voiron J 1985 *Phys. Rev.* B **32** 4822
[10] Oomi G and Mori N 1994 *J. Alloys Compounds* **207/208** 275
[11] Verbetskii V N, Kayumov R R and Semenenko K N 1991 *Izv. Akad. Nauk SSSR Metally* **6** 179 (in Russian)
[12] Bobet J L, Grigorova E, Chevalier B, Khrussanova M and Peshev P 2006 *Intermetallics* **14** 208
[13] Verbetsky V N and Movlaev E A 1997 *J. Alloys Compounds* **253/254** 38
[14] Kolomiets A V, Miliyanchuk K, Galadzhun Y, Havela L and Vejpravova J 2005 *J. Alloys Compounds* **402** 95
[15] Creuzet G and Gignoux D 1986 *Phys. Rev.* B **33** 515
[16] Marcano N, Gomez Sal J C, Espeso J I, De Teresa J M, Algarabel P A, Paulsen C and Iglesias J R 2007 *Phys. Rev. Lett.* **98** 166406

[17] Westlake D G, Shaked H, Mason P R, Mccart B R, Mueller M H, Matsumoto T and Amano M 1982 *J. Less-Common Met.* **88** 17
[18] Bowman R C, Adolphi N L, Hwang S J, Kulleck J G, Udovic T J, Huang Q and Wu H 2006 *Phys. Rev.* B **74** 184109
[19] Westlake D G 1980 *J. Less-Common Met.* **75** 177
[20] Isikawa Y, Mori K, Mizushima T, Fujii A, Takeda H and Sato K 1987 *J. Magn. Magn. Mater.* **70** 385
[21] Rajan V T, Lowenstein J H and Andrei N 1982 *Phys. Rev. Lett.* **49** 497
[22] Marcano N, Espeso J I, Gómez Sal J C, Rodríguez Fernández J, Herrero-Albillos J and Bartolomé F 2005 *Phys. Rev.* B **71** 134401
[23] Lazukov V N, Marcano N, Tiden N N, Espeso J I, Gómez Sal J C, Alekseev P A and Bewley R 2006 *Physica* B **378–380** 760
[24] Marcano N, Sal J C G, Espeso J I, Fernandez Barquin L and Paulsen C 2007 *Phys. Rev.* B **76** 224419
[25] Marcano N, Paccard D, Espeso J I, Allemand J, Moreau J M, Kurbakov A, Sekine C, Paulsen C, Lhotel E and Gómez Sal J C 2004 *J. Magn. Magn. Mater.* **272–276** 468
[26] Gignoux D and Gomez-Sal J C 1984 *Phys. Rev.* B **30** 3967
[27] Blanco J A, de Podesta M, Espeso J I, Gomezsal J C, Lester C, McEwen K A, Patrikios N and Rodríguez Fernández J 1994 *Phys. Rev.* B **49** 15126
[28] Isikawa Y, Mori K, Fujii A and Sato K 1986 *J. Phys. Soc. Japan* **55** 3165
[29] Sato K, Umehara I, Isikawa Y, Mori K and Takeda H 1993 *J. Appl. Phys.* **73** 6623
[30] Medina A N, Gandra F G, Azanha W R and Cardoso L P 1998 *J. Phys.: Condens. Matter* **10** 9763
[31] Chevalier B, Marcos J S, Fernandez J R, Pasturel M and Weill F 2005 *Phys. Rev.* B **71** 214437
[32] Chevalier B, Sebastian C P and Pöttgen R 2006 *Solid State Sci.* **8** 1000
[33] Chevalier B, Kahn M L, Bobet J L, Pasturel M and Etourneau J 2002 *J. Phys.: Condens. Matter* **14** L365–8
[34] Matar S F 2007 *Phys. Rev.* B **75** 104422
[35] Chevalier B, Gaudin E, Tencé S, Malaman B, Fernandez J R, Andre G and Coqblin B 2008 *Phys. Rev.* B **77** 014414
[36] Chevalier B and Matar S F 2004 *Phys. Rev.* B **70** 174408
[37] Chevalier B, Matar S F, Sanchez Marcos J and Rodriguez Fernandez J 2006 *Physica* B **378–380** 795
[38] Chevalier B, Gaudin E, Weill F and Bobet J L 2004 *Intermetallics* **12** 437
[39] Stewart G R 2001 *Rev. Mod. Phys.* **73** 797